Nrf2 in keratinocytes modulates UVB-induced DNA damage and apoptosis in melanocytes through MAPK signaling

Saowanee Jeayeng[a], **Adisak Wongkajornsilp**[a], **Andrzej T. Slominski**[b,c,d,e], **Siwanon Jirawatnotai**[a], **Somponnat Sampattavanich**[a], and **Uraiwan Panich**[a,*]

[a]Siriraj Laboratory for Systems Pharmacology, Department of Pharmacology, Faculty of Medicine Siriraj Hospital, Mahidol University, Bangkok 10700, Thailand [b]Department of Dermatology, University of Alabama at Birmingham, Birmingham, AL 35294, USA [c]Comprehensive Cancer Center, Cancer Chemoprevention Program, University of Alabama at Birmingham, Birmingham, AL 35294, USA [d]Nutrition Obesity Research Center, University of Alabama at Birmingham, Birmingham, AL 35294, USA [e]VA Medical Center, Birmingham, AL 35233, USA

Abstract

Responses of melanocytes (MC) to ultraviolet (UV) irradiation can be influenced by their neighbouring keratinocytes (KC). We investigated the role of Nrf2 in regulating paracrine effects of KC on UVB-induced MC responses through phosphorylation of MAPKs in association with oxidative stress in primary human MC cocultured with primary human KC using a transwell co-culture system and small-interfering RNA-mediated silencing of Nrf2 (siNrf2). The mechanisms by which Nrf2 modulated paracrine factors including α-melanocyte-stimulating hormone (α-MSH) and paracrine effects of KC on UVB-mediated apoptosis were also assessed. Our findings showed that co-culture of MC with siNrf2-transfected KC enhanced UVB-mediated cyclobutane pyrimidine dimer (CPD) formation, apoptosis and oxidant formation, together with phosphorylation of ERK, JNK and p38 in MC. Treatment of MC with conditioned medium (CM) from Nrf2-depleted KC also increased UVB-mediated MC damage, suggesting that KC modulated UVB-mediated MC responses via paracrine effects. Additionally, depletion of Nrf2 in KC suppressed UVB-induced α-MSH levels as early as 30 min post-irradiation, although pretreatment with N-acetylcysteine (NAC) elevated its levels in CM from siNrf2-transfected KC. Furthermore, NAC reversed the effect of CM from Nrf2-depleted KC on UVB-induced apoptosis and inflammatory response in MC. Our study demonstrates for the first time that KC provided a rescue effect on UVB-mediated MC damage, although depletion of Nrf2 in KC reversed its protective effects on MC in a paracrine fashion in association with elevation of ROS levels and activation of MAPK pathways in MC. Nrf2 may indirectly regulate the paracrine effects of KC probably by affecting levels of the paracrine factor α-MSH via a ROS-dependent mechanism.

*Correspondence to: Department of Pharmacology, Faculty of Medicine Siriraj Hospital, Mahidol University, 2 Prannok Rd., Bangkoknoi, Bangkok 10700, Thailand. uraiwan.pan@mahidol.ac.th (U. Panich).

Conflicts of interest

No conflicts of interest were declared in relation to this article.

Keywords

Nuclear factor E2-related factor 2 (Nrf2); Keratinocytes; Ultraviolet B; Apoptosis; Melanocytes; Reactive oxygen species (ROS)

1. Introduction

Ultraviolet radiation (UVR) is detrimental to human skin through triggering various types of cellular damage, most notably DNA damage and oxidative damage, and thus has been accepted as human carcinogen accountable for increased risk of developing skin cancers including cutaneous melanoma [1,2]. UVB irradiation can cause the loss of cellular integrity, direct damage to DNA and trigger various cellular responses including apoptosis [3] and inflammation [4] in skin cells including melanocytes (MC). However, biological and physiological responses of normal MC to UVR are complex and regulated by various factors secreted by their neighbouring cells including keratinocytes (KC) for maintenance of MC homeostasis [5–7]. Microenvironmental conditions created by KC play a role in regulation of MC responses including apoptosis and cellular damage induced by UVR through secretion of paracrine factors such as endothelin-1 (ET-1) and hypothalamic and pituitary peptides such as proopiomelanocortin (POMC) derived adrenocorticotropic hormone, β-endorphin and α-melanocyte-stimulating hormone (α-MSH) or corticotropin releasing hormone (CRH) [8–12] or other regulatory biomolecules [13]. α-MSH has been recognized as a crucial paracrine factor playing a protective role against UVB radiation-induced apoptosis and DNA damage in human MC [8,14]. It is also suggested that cytoprotective effects of α-MSH against UVR-mediated photodamaged skin were attributed to their abilities to suppress apoptosis, oxidative stress and the inflammatory response [15]. However, the mechanism involved in regulation of KC's paracrine effects affecting MC activity has not been investigated.

Nuclear factor E2-related factor 2 (Nrf2) is a master transcription factor regulating several phase II detoxification and antioxidant genes involved in cellular defenses against oxidative stress and environmental insults. Nrf2 has been suggested to play a regulatory role in UVR-mediated oxidative stress associated with disturbance in physiology of the skin cells including MC [16,17]. Additionally, Nrf2 has been demonstrated to be involved in regulation of paracrine factors such as epidermal growth factor family member epigen in KC causing sebaceous gland enlargement in mice [18]. Since modulation of Nrf2 can affect KC's function involving their paracrine effects in response to UVR, we thus address whether Nrf2 in KC had an impact on the microenvironment created by KC in regulation of MC responses to UVB exposure. Moreover, UVB irradiation could mediate apoptosis via oxidative stress-dependent activation of upstream mitogen activated protein kinases (MAPKs) in MC and KC [19,24]. We thus determined whether modulation of Nrf2 can affect paracrine activity of KC on UVB-mediated CPD formation and apoptosis in primary human MC. Phosphorylation of MAPKs (ERK, JNK and p38) and oxidative stress were also concurrently monitored. We investigated these questions by co-culturing primary human KC with primary human MC using a transwell co-culture system. Alternatively, MC were incubated with conditioned medium (CM) which were prepared from siRNA against Nrf2

(siNrf2)-transfected KC. Silencing of Nrf2 in KC was employed to confirm the role of Nrf2 in modulating paracrine activity of KC on UVB-mediated MC damage. In MC, we monitored how paracrine action of KC affected apoptosis and inflammatory response following UVB exposure. Finally, we explored the underlying mechanism by which Nrf2 regulated secretion of α-MSH and paracrine effects of KC on MC's inflammatory responses including the activity of NF-κB signaling cascade and the release of TNF-α.

2. Materials and methods

2.1. Cell culture

Primary human epidermal melanocytes (MC) and primary human epidermal keratinocytes (KC) were obtained from Invitrogen (NY, USA). MC were cultured in Medium 254 (#M-254-500) supplemented with human melanocyte growth supplement (HMGS) according to the manufacturer's instructions. KC were cultured in Medium 154 (#M-154CF-500) supplemented with human keratinocyte growth supplement (HKGS). All cells were maintained at 37 °C in a humidified air of 5% CO_2 (PCO2=40 Torr) (a Forma Scientific CO_2 Water Jacketed Incubator).

2.2. Double transfection with small interfering RNA (siRNA) against Nrf2 in KC

A combination of four gene-specific small interfering RNA (siRNA) against human Nrf2 (NM_006164) was used (FlexiTube GeneSolution GS4780 for NFE2L2, Qiagen; Cat.#: 1027416). KC were initially transfected with 5 nM siRNA against Nrf2 (siNrf2) or equal molar non-silencing siRNA controls (siCtrl, Qiagen; Cat.#:1022076) using HiPerFect transfection reagent (Qiagen; Cat.#: 301705) according to the manufacturer's instructions as previously described [16]. At 48 h after the first transfection, cells were retransfected for the second time with siNrf2 or siCtrl at the same concentration using the same protocol described above. At 96 h following the first transfection, the transfected KC were used for further experiments.

2.3. MC-KC co-culture in transwell systems

MC were co-cultured with KC or the transfected KC at a ratio of 1:5 MC to KC in 6-well transwell plates for 24 h. MC were seeded at a density of 6×10^4 cells on the insert layer of Corning transwell plates with 0.4-μm pore polycarbonate membranes whereas KC were grown in the bottom well.

2.4. UVB irradiation and treatment of cells

After a 24 h period of co-culture, both MC and KC were irradiated separately with UVB under a thin layer of Dulbecco's phosphate buffered saline (DPBS). The culture plates were exposed for 22 s, 45 s or 1 min 30 s to achieve a single dose of 62.5, 125 or 250 mJ/cm², respectively. The UV intensity determined at a distance of 21 cm from the UVB lamp was 1 W/cm² using a UV-meter (Dr Honle, Martinsried, Germany) equipped with UVB sensor (290–320 nm). Immediately after UVB exposure, DPBS was replaced with Medium 254 without HMGS for MC and Medium 154 without HKGS for KC to continue the co-culture in the same transwell. Then, MC were harvested at different time points as indicated in results.

To determine whether Nrf2 knockdown in KC affected gene expression and secretion of important paracrine factors, we determined mRNA levels of corticotropin-releasing hormone (CRH), corticotropin-releasing hormone receptor 1 (CRHR1), endothelin-1 (ET-1) and proopiomelanocortin (POMC) at 30 min and 3 h following UVB exposure using real time RT-PCR and levels of α-MSH in CM from KC at 15 and 30 min, 3, 6 and 12 h post-irradiation using a commercial ELISA kit. To assess whether Nrf2-modulated the paracrine factors and effect of KC involved a ROS-dependent mechanism, siCtrl- and siNrf2-transfected KC were incubated with 5 mM N-acetylcysteine (NAC), a well-known ROS scavenger, in Medium 154 without HKGS for 24 h and the medium was replaced with DPBS prior to UVB exposure. Then, ROS generation and α-MSH levels in CM from siCtrl- and siNrf2-transfected KC with or without NAC pretreatment were determined at 30 min following UVB exposure. For detection of apoptosis, active caspase-3 and phosphorylation of p53 induced by UVB (250 mJ/cm^2) were determined following irradiation at 12 h and 15 min, respectively, in MC incubated with CM from Nrf2-depleted KC with or without NAC pretreatment. Whether the paracrine effect of KC involved protection against UVB (125 mJ/cm^2)-mediated inflammatory response in MC was also assessed by detection of NF-κB activation indicated by nuclear:cytosolic ratio of NF-κB p65 and p50 subunits at 6 h post-irradiation and TNF-α levels at 24 h post-irradiation.

2.5. Preparation of KC-derived conditioned medium (KC-CM)

KC or the transfected KC were seeded at a density of 3×10^5 cells/well in 6-well plates. Conditioned-KC supernatants were prepared by irradiation of KC or the transfected KC in DPBS with UVB (62.5–250 mJ/cm^2) and this DPBS were collected at 30 min post-irradiation and used as KC-CM for treatment of MC. MC was pre-incubated with KC-CM for 30 min, subjected to UVB irradiation and harvested at 1 h for determination of CPD and ROS formation and 12 h for caspase-3 activation.

2.6. Determination of cyclobutane pyrimidine dimer (CPD) photoproducts by ELISA

MC were irradiated with UVB (125 mJ/cm^2) and harvested at 1 h post-irradiation. Genomic DNA was then extracted using a spin-column based genomic DNA isolation kit (GET™ DNA Template) (G-Bioscience, St Louis, MO, USA) according to the protocol's instruction. The CPD in genomic DNA was measured by Oxiselect oxidative DNA damage ELISA kit (Cell Biolabs, San Diego, CA). The CPD was detected with an anti-CPD antibody, followed by incubation with horseradish peroxidase (HRP)-conjugated secondary antibody.

2.7. Annexin V/PI (propidium iodide) staining

Determination of phosphatidylserine on the outer leaflet of apoptotic cells was employed using annexin-V binding and PI according to the manufacturer's instructions (BD Biosciences, USA). Briefly, MC were stained with annexin V-APC and 3 μg/ml PI and analyzed by flow cytometry using a fluorescence activated cell sorter (FACS-calibur). Apoptosis was determined by the relative amount of APC+ PI- cell populations.

2.8. Measurement of active caspase-3

Active caspase-3 was measured using PE Active Caspase-3 Apoptosis Kit (BD Biosciences, USA) according to the manufacturer's instructions. Briefly, MC were fixed and permeabilized using the Cytofix/CytopermTM for 30 min, pelleted and washed with Perm/WashTM Buffer. Cells were subsequently stained with the rabbit anti-active caspase-3 antibody (clone C92-605) (BD Biosciences, USA) in the dark. Cells were then washed and resuspended in Perm/WashTM Buffer and analyzed by flow cytometry.

2.9. Determination of intracellular oxidant formation by flow cytometry

The assay is based on conversion of non-fluorescent dichlorofluorescein (H2DCFDA) to the fluorescent 2,7-DCF upon oxidation by intracellular ROS. After treatment, MC were washed and incubated with Medium 254 without HMGS for 30 min. Then, cells were incubated in DPBS with 5 μM H_2DCFDA at 37 °C for 30 min and analyzed by flow cytometery using a fluorescence activated cell sorter (FACS-calibur).

2.10. Measurement of cellular antioxidant defenses

GSH assays were carried out using the glutathione reductase (GSSG): (5,5′-dithio-bis-2-(nitrobenzoic acid)) (DTNB) enzymatic recycling method following the kit protocol from Sigma-Aldrich (MO, US) as previously described [20] and GSH levels expressed as nmol/mg protein. Catalase (CAT) is involved in the neutralization of hydrogen peroxide (H_2O_2). Its activity was measured following the kit protocol from Cayman chemical (Ann Arbor, MI) as previously described [20] and CAT activity expressed as unit/mg protein. Superoxide dismutase (SOD) activity assay was performed following the kit protocol from Cayman chemical (Ann Arbor, MI) and the method of Johns et al. [21,22] with some modifications as previously described [20]. Total SOD activity was expressed in unit/mg protein.

2.11. Western blot analysis

Western blot analysis was performed to examine Nrf2 knockdown efficiency using double transfection of KC with Nrf2-siRNA and detect phosphorylated MAPKs (ERK, JNK, and p38) in MC. Total protein extracts were prepared as previously described [16]. The membranes were blocked in 5% (w/v) skim milk in Tris-buffered saline containing 0.1% (v/v) Tween 20 for 1.5 h and incubated at 4 °C overnight with the primary antibody against Nrf2 (sc-722; Santa Cruz Biotechnology, Santa Cruz, CA) (1:2000), phosphorylated Erk1/2 (p44/42 MAPK (Thr202/Tyr204) (4370S; Cell Signaling) (1:2000), phosphorylated JNK (Thr183/Tyr185) (G9) (9255S; Cell Signaling) (1:1000), phosphorylated p38 (Thr180/Tyr182) (D3F9) (4511S; Cell Signaling) (1:1000), p65 (Sc-109; Santa Cruz Biotecnology) (1:1000) and p50 (Sc-114; Santa Cruz Biotecnology) (1:1000) subunits of NF-κB, phospho-p53 (Ser15) (9284; Cell Signaling) (1:1000) and p53 (2524; Cell Signaling) (1:1000), in 5% skim milk. The membranes were washed with a PBS solution and incubated for 1.5 h at room temperature with the HRP-conjugated secondary antibodies (ab6789 for anti-mouse and ab6721 for anti-rabbit HRP labelled secondary antibody; Abcam, Cambridge, MA, USA) (1:2000) in 5% skim milk. Immunoreactivity is detected using the Bio-Rad Clarity western ECL (Bio-Rad). Protein bands were visualized using an ImageQuant LAS 4000

digital imaging system (GE Healthcare, UK) and analyzed as previously described [16]. The protein expressions were normalized to expression of loading controls; α-Tubulin (ab7291; Abcam, Cambridge, MA, USA) (1:5000) for Nrf2 protein in whole cell lysates, total ERK protein (p44/42 MAPK) (Erk1/2) (4695 S; Cell Signaling) for phosphorylated ERK, total JNK protein (9252S; Cell Signaling) for phosphorylated JNK, total p38 protein (9212S; Cell Signaling) (1:2000) for phosphorylated p38, βactin (A3854; Sigma) (1:10000) for cytosolic p65 and p50 subunits of NF-κB and phospho-p53 (Ser15) and lamin A (sc-20680, Santa Cruz Biotecnology) (1:1000) for nuclear p50 and p65 subunits of NF-κB.

2.12. Quantitative real-time reverse transcriptase-polymerase chain reaction (RT-PCR) for determination of mRNA expression

mRNA levels of Nrf2 and its target genes, CRH, CRHR1, ET-1 and POMC were determined by RT-PCR. Total RNA was isolated using the illustra RNAspin Mini RNA Isolation Kit (GE Healthcare, UK) and reverse transcription was carried out using the Improm-II reverse transcriptase (Promega, Medison, USA) under the conditions described in the kit manual. Primers for PCR were designed using the Primer Express software version 3.0 (Applied Biosystems, USA). Sequences of PCR primer (in $5' \rightarrow 3'$ direction) were as follows: CRH (product sizes =144 bp) sense, CTCCGGGAAGTCTTGGAAAT, and antisense, GTTGCTGTGAGCTTGCTGTG; CRHR1 (product sizes =100 bp) sense, TGGATGTTCATCTGCATTGG, and antisense, TGCCAAACCA GCACTTCTC; ET-1 (product sizes =274 bp) sense, TCTACTTCTGCCACCTGGAC, andantisense, CACTTCTTTCCCAACTTGG AAC; POMC, exon 3 (product sizes =152 bp) sense, AGCCTCAGCCTGCCTGGAA, and antisense, CAGCAGGTTGCTTTCC GTGGTG [23]. Primer sets of Nrf2 target genes were previously described [16]. The mRNA level was calculated by normalizing with the expression level of GAPDH mRNA. The mean Ct from mRNA expression in cDNA from each sample was compared with the mean Ct from GAPDH determinations from the same cDNA samples.

2.13. Determination of α-MSH and TNF-α levels by ELISA

α-MSH and TNF-α levels in culture supernatants were determined using competitive enzyme immunoassay kits from EK-043-01, Phenix Pharmaceuticals Inc., Hayward, CA, USA, and EH3TNFA, Thermo Scientific, Rockford, IL, USA, respectively, according to the manufacturer's instructions. Sample or α-MSH standards were added to the immunoplate pre-coated with secondary antibody. An anti-α-MSH antibody was added, followed by biotinylated peptide. Biotinylated peptide then interacted with streptavidin-horseradish peroxidase (HRP), which catalyzed the substrate solution. For measurement of TNF-α levels, sample or the standard were added to an anti-human TNF-α precoated plate. Streptavidin HRP was used to detect bound antibodies and tetramethylbenzidine was used as a substrate for the color development, which was stopped with 0.16 M sulfuric acid. α-MSH and TNF-α levels were determined by comparison with the standard curve.

2.14. Statistical analysis

Data are expressed as mean ± standard deviation of the mean (SD) of at least three separate experiments (n 3) performed on different days using freshly prepared reagents. Statistical significance of differences between different groups was evaluated by independent t-test

(Student's; 2 populations) or one-way analysis of variance (ANOVA) followed by Tukey or Dunnett tests, where appropriate, using Prism (GraphPad Software Inc., San Diego, CA).

3. Results

3.1. SiRNA knockdown of Nrf2 in KC is associated with induction of UVB-mediated CPD formation in MC co-cultured with KC

We employed a transwell co-culture system to avoid effects of cell-cell contact to determine whether non-contact co-culture of primary human MC with primary human KC modulated UVB-mediated CPD formation in MC. In addition, to confirm that microenvironment created by KC affected formation of CPD in MC, CM derived from UVB-irradiated KC was used to treat MC. Here, we first observed that UVB (125 mJ/cm^2) irradiation caused a substantial production of CPD photoproducts in MC monoculture from 30 to 120 min (Fig. 1A). However, an approximately 2-fold decrease in CPD formation was found in both MC co-cultured in transwell with KC and in MC pretreated with CM from irradiated KC compared to MC monoculture subjected to UVB challenge (Fig. 1B).

We also explored whether depletion of Nrf2 in KC using siNrf2 would affect UVB-mediated DNA damage in MC. The efficiency of Nrf2 silencing in KC was verified by real-time RT-PCR and western blot analysis at 96 h after the initial transfection with either siNrf2 or siCtrl. Nrf2 knockdown efficiency of ~70% was achieved at mRNA and protein levels (Supplementary Fig. 1A). A substantial reduction of Nrf2 target genes including GCL, GST and NQO1 by ~ 60% (Supplementary Fig. 1B) was observed in siNrf2-transfected KC compared with untransfected and siCtrl-transfected KC. Furthermore, enhanced yield of UVB-induced CPD DNA lesions was demonstrated in MC co-cultured with Nrf2-depleted KC and in MC treated with CM derived from Nrf2-depleted KC compared to MC co-cultured with siCtrl-transfected KC or MC treated with CM from siCtrl-transfected KC, suggesting that Nrf2 might play a role in the protective effects of KC probably acting in a paracrine fashion against UVB-induced CPD formation in MC. Moreover, our results revealed that, upon UVB irradiation, increased levels of CPD in MC co-cultured with siNrf2-transfected KC or in MC treated with CM derived from siNrf2-transfected KC were comparable to those in UVB-irradiated MC monoculture.

3.2. SiRNA knockdown of Nrf2 in KC is associated with induction of UVB-mediated apoptosis in MC co-cultured with KC

To evaluate whether Nrf2 in KC influenced the microenvironment created by KC on UVB-induced apoptosis, we first demonstrated that, at 12 h post-irradiation, UVB irradiation resulted in a significant induction of annexin V positivity (Fig. 2A) and active caspase-3 (Fig. 2B), the well-known hallmarks of apoptosis, in MC monoculture, although UVB-mediated apoptosis was rescued when co-cultured in transwell with KC. As shown in Fig. 2C, UVB-mediated active caspase-3 was remarkably reduced in MC treated with CM from UVB-irradiated KC compared with untreated MC monoculture. Moreover, partial knockdown of Nrf2 significantly suppressed rescue effect of the microenvironment created by KC on UVB-induced apoptotic cell death because annexin-V staining (Fig. 2D) and caspase-3 activation (Fig. 2E) were markedly enhanced in MC co-cultured in transwell with

siNrf2-transfected KC compared to MC co-cultured with siCtrl-transfected KC following UVB irradiation. In addition, MC treated with CM from Nrf2-depleted KC revealed greater active caspase-3 levels than those in the cells treated with CM from siCtrl-transfected KC and the levels of active caspase-3 were comparable to those in UVB-irradiated MC monoculture (Fig. 2E).

3.3. Suppression of UVB-induced ROS formation and depletion of antioxidant defenses in MC co-cultured with KC: modulation by SiRNA knockdown of Nrf2 in KC

We determined intracellular ROS formation and antioxidant defense systems including glutathione (GSH) levels and activities of catalase and superoxide dismutase (SOD) to delineate the role of KC acting in a paracrine fashion against UVB-mediated apoptosis in association with modulation of redox status in MC. Decreased ROS formation (Fig. 3A) and increased antioxidant defenses (GSH levels and activities of catalase and SOD) (Fig. 3B) were observed in MC co-cultured in transwell with irradiated KC compared to MC monoculture in response to UVB irradiation. We also confirmed that KC was responsible for the protective actions against UVB-mediated cellular oxidative stress in MC via paracrine effects upon stimulation with UVB because treatment of MC with CM from KC irradiated with UVB (125 and 250 mJ/cm^2) significantly abrogated UVB-induced ROS formation when compared to irradiated MC without CM treatment (Fig. 3A). We also demonstrated that Nrf2 in KC may affect their microenvironment via regulation of oxidative stress in MC because elevated ROS formation was found in irradiated MC pretreated with CM from siNrf2-transfected KC but not in the MC pretreated with CM from siCtrl-transfected KC (Fig. 3C), indicating that depletion of Nrf2 in KC reversed its protective effects on oxidative stress in MC.

3.4. SiRNA knockdown of Nrf2 in KC is associated with induction of UVB-mediated MAPK signaling in MC co-cultured with KC

We have hypothesized that the microenvironment created by KC regulated UVB-induced MC apoptosis through an involvement of the MAPK pathway. UVB irradiation was observed to cause a pronounced transient induction of p-ERK, p-JNK and p-p38 in MC at as early as 5 min following UVB irradiation (Fig. 4A). Moreover, the role of MAPKs in regulation of UVB-induced apoptosis in MC was examined by determination of active caspase-3 in MC treated with specific inhibitors of ERK, JNK and p38 MAPK pathways following UVB irradiation (250 mJ/cm^2). Our findings revealed that treatment with 1 μM U0126 (a selective inhibitor of ERK), SP600125 (a selective inhibitor of JNK) and SB203580 (a selective inhibitor of p38) markedly reduced caspase-3 activation in irradiated MC compared to irradiated cells without the MAPK inhibitors (Fig. 4B). We then assessed whether Nrf2 in KC affected responses of MC to UVB irradiation in association with MAPK signaling. Our results demonstrated a significant reduction of p-ERK, p-JNK and p-p38 levels in MC co-cultured with irradiated KC compared to MC monoculture in response to UVB challenge, although co-culture with siNrf2-transfected KC led to elevated levels of p-ERK, p-JNK and p-p38 in MC in response to UVB exposure, suggesting that the rescue effects of KC on UVB-induced MAPK phosphorylation in MC was reversed by Nrf2 depletion (Fig. 4C).

3.5. Modulation by Nrf2 knockdown of the paracrine factor α-MSH produced by KC is ROS-dependent

We next investigated the mechanisms by which Nrf2 modulated paracrine factors produced by KC and observed that UVB irradiation did not affect mRNA levels of the paracrine factors (CRH, CRHR1, ET-1 and POMC) at 30 min and 3 h post-irradiation in both siCtrl- and siNrf2-transfected KC (Fig. 5A). However, UVB irradiation enhance α-MSH levels in CM from siCtrl-transfected KC (Fig. 5B) as early as 15 min after irradiation and increasing up to 12 h but reduce α-MSH levels in the CM from Nrf2-depleted KC. Moreover, when we reduced the level of ROS in CM by pretreating KC with NAC, a well-known ROS scavenger, α-MSH levels were found to be elevated in CM from siNrf2-depleted KC (Fig. 5C).

3.6. Modulation by Nrf2 knockdown of KC's paracrine effect on apoptosis and inflammatory response in MC is ROS-dependent

To address whether a ROS-dependent mechanism was involved in Nrf2-modulated paracrine effect of KC on UVB-mediated MC damage, we first confirmed an enhanced formation of ROS in siNrf2-transfected KC compared to siCtrl-transfected KC in response to UVB irradiation and increased ROS levels could be rescued by NAC treatment (Supplementary Fig. 2). Our study determined active caspase-3 and phosphorylation of p53 because caspase-3 is known as the critical driver of apoptotic cell death and both caspase-3 and p53 could mediate apoptosis in association with UVB-induced DNA damage in skin cells (including KC and MC) [25,26]. Our findings revealed that modulation by Nrf2 of KC's protective effect on UVB-induced apoptosis in MC is ROS-dependent because NAC could reverse the effect of CM from Nrf2-depleted KC on UVB ($250 \ mJ/cm^2$)-induced caspase-3 activation (Fig. 6A) and phosphorylation of p53 (Fig. 6B). To address whether inflammatory response was associated with UVB-induced MC damage, we determined activation of NF-κB, a major transcription factor regulating proinflammatory signaling, and levels of TNF-α, a crucial proinflammatory cytokine involved in UVB-induced MC damage. Irradiation of MC with UVB ($125 \ mJ/cm^2$) irradiation was observed to cause a substantial induction of nuclear/cytosolic ratio of NF-κB p65 (Fig. 7A) and p50 (Fig. 7B) subunits indicating NF-κB activation and levels of TNF-α (Fig. 7C) produced by MC incubated with CM from siNrf2-transfected KC compared to MC incubated with CM from siCtrl-transfected KC. However, pretreatment of Nrf2-depleted KC with NAC was shown to rescue KC's protective effects on UVB-induced NF-κB activity and TNF-α release in MC (Fig. 7A–C), indicating that Nrf2 modulated paracrine effect of KC on UVB-mediated inflammatory response in MC via a ROS-dependent mechanism.

4. Discussion

Under both physiological and pathological conditions including epidermal photodamage, the homeostasis of human MC is regulated and maintained by a complex paracrine networks of KC and MC derived factors acting in reciprocal fashion. In addition, oxidative stress can disrupt the homeostasis of epidermal MC through damage to the DNA, proteins and interference with cell signaling, leading to cell death, apoptosis or malignant transformation [27,28]. Nrf2 has been suggested to play a protective role in UVR-mediated oxidative stress accountable for impaired physiology and function of the skin cells including MC [16,17,29].

Our study revealed that UVB-induced CPD formation and apoptosis in MC was suppressed by co-culture with KC. The co-culture with KC also reversed UVB-mediated formation of ROS and impairment of antioxidant defense capacity in MC. In addition, pretreatment with CM from irradiated KC prior to UVB exposure attenuated caspase-3 activation and ROS formation in MC, suggesting that suppression of UVB-dependent cell responses of MC probably involved paracrine factors produced by KC upon UVB stimulation. These results indicate a rescue effect of KC on UVB-induced CPDs and apoptosis in association with disturbance of redox status in MC. They are in agreement with previous studies indicating protective effects of KC against UVB-induced pathologies including DNA damage, apoptosis and melanogenesis in MC [30–34]. Proposed mechanisms responsible for the role of neighbouring KC in mediating UVB-stimulated physiological responses of MC in association with inhibition of oxidative stress would likely involve the paracrine effects of factors produced by epidermal KC [7,9,10,13,35,36]. We therefore addressed the role of Nrf2 in modulation of KC's paracrine effects on UVB-mediated MC damage. Our findings reveal that a partial knockdown of Nrf2 in KC reversed the protective effects of microenvironment created by KC on UVB-induced CPD formation and apoptosis in MC. Furthermore, the paracrine rescue effects of KC against UVB-stimulated CPD level, active caspase-3 and ROS formation in MC were confirmed using CM from UVB-irradiated KC, revealing that cellular oxidative stress accompanying DNA damage and apoptotic responses of MC may be induced by altered microenvironment created by Nrf2-depleted KC. UVB irradiation has been suggested to initiate phosphorylation of MAPKs in association with induction of DNA damage and apoptosis in MC [24,37]. In this study, we found that ERK, JNK and p38 MAPK pathways play a role in UVB-mediated MC apoptosis. Furthermore, non-contact co-culture of MC with KC following UVB irradiation showed reduced phosphorylation of ERK, JNK and p38 MAPKs, although depletion of Nrf2 in KC reversed their inhibitory effects on UVB-induced phosphorylation of MAPKs in MC co-cultured with siNrf2-transfected KC pre-irradiated with UVB. Therefore, we proposed that microenvironment created by KC regulated UVB-induced MC apoptosis through an involvement of the MAPK pathway. Activation of MAPKs in response to different stress stimuli mediates apoptosis via several mechanisms including activation of caspases, release of proapoptotic factors (such as cytochrome c) from mitochondria, induction of p53 and transcriptional activation of apoptotic genes [38–40]. In our study, inhibition of MAPKs may suppress apoptosis at least partially through downregulation of caspase-3 activation.

Genetic silencing of Nrf2 in KC without UVB exposure did not affect the responses of MC co-cultured with siNrf2-transfected KC. It should also be noted that levels of active caspase-3 and ROS induced by UVB were similar in MC monoculture and in MC treated with CM from unirradiated KC (Supplementary Fig. 3), implying that UVB irradiation was required to induce KC-derived rescue mechanism against MC damage. Our observations further suggest that Nrf2 modulated paracrine factors produced by KC and their protective effects on UVB-mediated MC damage via a ROS-dependent mechanisms. In our study using CM collected from KC at 30 min after UVB exposure to treat MC, modulation of the paracrine factors and effects by Nrf2 seems to occur independent of transcriptional control of paracrine factors including CRH, CRHR1, ET-1 and POMC. Our findings suggested that Nrf2 might modulate paracrine factors produced by KC via a ROS-dependent mechanism

because NAC pretreatment can restore α-MSH levels in Nrf2-depleted KC in response to UVB exposure. Crucial biological responses of MC to UVB irradiation-mediated oxidative stress include apoptosis and inflammation. ROS have been shown to activate proinflammatory and MAPK signaling cascades, subsequently leading to various biological responses including cell death or dysfunction [43–45]. López et al., reported that paracrine protective effects of CM from UVB-irradiated KC on MC involved regulation of various signaling pathways including proinflammatory and p53-dependent apoptotic pathways [42]. Our study demonstrated that the microenvironment created by KC reversed damaging effects of UVB on MC by reducing activation of caspase-3 and p53 that play a crucial role in UVR-mediated apoptosis associated with DNA damage [25,26], and by downregulating inflammatory markers including NF-κB activation and TNF-α levels implicated in photodamaged skin [46,47]. Nevertheless, depletion of Nrf2 in KC resulted in suppression of its protective effects on UVB-mediated DNA damage, apoptosis and inflammatory response in MC. Furthermore, the mechanism by which Nrf2 supported paracrine protection by KC against UVB damage might be ROS-dependent as pretreatment of Nrf2-depleted KC with NAC could recover the impaired paracrine effects of KC on UVB-induced apoptosis and inflammatory response in MC. Recently, oxidative stress was suggested to compromise paracrine protective effect of KC through upregulation of microRNA-25 [41]. Upon stress insults, ROS induced by Nrf2 depletion could modulate paracrine effects and several signaling cascades, which subsequently affect UVB response of MC. It should be also taken into account that while Nrf2 plays a crucial role in maintaining cellular homeostasis and cytoprotection against stress stimuli, a harmful aspect of Nrf2 defined as the "dark side of Nrf2" in the skin and cancer biology, has been widely discussed. Previous *in vivo* studies demonstrated that prolonged activation of Nrf2 in KC resulted in sebaceous gland enlargement and seborrhea [48]. Moreover, resistance to apoptosis induced by UVB associated with failure in removing unstable or damaged cells is recognized as a common feature of melanoma [49,50]. Thus, the role of Nrf2 in modulating production and secretion of KC's paracrine factors and whether its role in supporting the protective effects of KC against UVB-induced apoptosis can be implicated in carcinogenesis of melanoma needs further investigations.

In summary, KC provided a rescue effect on UVB-induced CPDs, apoptosis and inflammatory responses in MC, although depletion of Nrf2 in KC reversed its protective effects on MC in a paracrine fashion. This was associated with an elevation of ROS levels and an activation of MAPK pathways in MC. Nrf2 may indirectly modulate the paracrine effects of KC by regulating levels of their paracrine factors via a ROS-dependent mechanism.

Supplementary Material

Refer to Web version on PubMed Central for supplementary material.

Acknowledgments

Abbreviations

CM	conditioned medium
CPD	cyclobutane pyrimidine dimer
CRH	corticotropin releasing hormone
CRHR1	corticotropin releasing hormone receptor 1
ET-1	endothelin-1
KC	keratinocytes
MAPKs	mitogen-activated protein kinases
MC	melanocytes
α-MSH	alpha-melanocyte-stimulating hormone
Nrf2	nuclear factor E2-related factor 2
POMC	pro-opiomelanocortin
ROS	reactive oxygen species
siCtrl	non-silencing siRNA controls
siNrf2	siRNA against Nrf2
TNF-α	tumor necrosis factor-alpha
UVB	ultraviolet B

References

1. Agar N, Young AR. Melanogenesis: a photoprotective response to DNA damage? Mutat Res. 2005; 571:121–132. [PubMed: 15748643]

2. Brozyna A, Zbytek B, Granese J, Carlson JA, Ross J, Slominski A. Mechanism of UV-related carcinogenesis and its contribution to nevi/melanoma. Expert Rev Dermatol. 2007; 2:451–469. [PubMed: 18846265]

3. Premi S, Wallisch S, Mano CM, Weiner AB, Bacchiocchi A, Wakamatsu K, Bechara EJ, Halaban R, Douki T, Brash DE. Chemiexcitation of melanin derivatives induces DNA photoproducts long after UV exposure. Science. 2015; 347:842–847. [PubMed: 25700512]

4. Gledhill K, Rhodes LE, Brownrigg M, Haylett AK, Masoodi M, Thody AJ, Nicolaou A, Tobin DJ. Prostaglandin-E2 is produced by adult human epidermal melanocytes in response to UVB in a melanogenesis-independent manner. Pigment Cell Melanoma Res. 2010; 23:394–403. [PubMed: 20236442]

5. Bowen AR, Hanks AN, Allen SM, Alexander A, Diedrich MJ, Grossman D. Apoptosis regulators and responses in human melanocytic and keratinocytic cells. J Invest Dermatol. 2003; 128:48–55.

6. Coleman DJ, Chagani S, Hyter S, Sherman AM, Löhr CV, Liang X, Ganguli-Indra G, Indra AK. Loss of keratinocytic RXRalpha combined with activated CDK4 or oncogenic NRAS generates

UVB-induced melanomas via loss of p53 and PTEN in the tumor microenvironment. Mol Cancer Res. 2015; 13:186–198. [PubMed: 25189354]

7. Slominski A, Zmijewski MA, Skobowiat C, Zbytek B, Slominski RM, Steketee JD. Sensing the environment: regulation of local and global homeostasis by the skin neuroendocrine system. Adv Anat Embryol Cell Biol. 2012; 212:1–115.

8. Bohm M, Wolff I, Scholzen TE, Robinson SJ, Healy E, Luger TA, Schwarz T, Schwarz A. alpha-Melanocyte-stimulating hormone protects from ultraviolet radiation-induced apoptosis and DNA damage. J Biol Chem. 2005; 280:5795–5802. [PubMed: 15569680]

9. Hyter S, Coleman DJ, Ganguli-Indra G, Merrill GF, Ma S, Yanagisawa M, Indra AK. Endothelin-1 is a transcriptional target of p53 in epidermal keratinocytes and regulates ultraviolet-induced melanocyte homeostasis. Pigment Cell Melanoma Res. 2013; 26:247–258. [PubMed: 23279852]

10. Kadekaro AL, Kavanagh R, Kanto H, Terzieva S, Hauser J, Kobayashi N, Schwemberger S, Cornelius J, Babcock G, Shertzer HG, Scott G, Abdel-Malek ZA. Alpha-Melanocortin and endothelin-1 activate antiapoptotic pathways and reduce DNA damage in human melanocytes. Cancer Res. 2005; 65:4292–4299. [PubMed: 15899821]

11. Slominski A, Wortsman J, Luger T, Paus R, Solomon S. Corticotropin releasing hormone and proopiomelanocortin involvement in the cutaneous response to stress. Physiol Rev. 2000; 80:979–1020. [PubMed: 10893429]

12. Slominski A, Zmijewski M, Zbytek B, Tobin DJ, Theoharides TC, Rivier J. Key role of CRF in the skin stress response system. Endocr Rev. 2013; 34:827–884. [PubMed: 23939821]

13. Slominski A, Wortsman J, Tobin DJ. The cutaneous serotoninergic/melatoninergic system: securing a place under the sun. FASEB J. 2005; 19:176–194. [PubMed: 15677341]

14. Swope VB, Abdel-Malek Z. Significance of the melanocortin 1 and endothelin B receptors in melanocyte homeostasis and prevention of sun-induced genotoxicity. Front Genet. 2016; 7:146. [PubMed: 27582758]

15. Böhm M, Luger TA, Tobin DJ, García-Borrón JC. Melanocortin receptor ligands: new horizons for skin biology and clinical dermatology. J Investig Dermatol. 2006; 126:1966–1975. [PubMed: 16912693]

16. Chaiprasongsuk A, Onkoksoong T, Pluemsamran T, Limsaengurai S, Panich U. Photoprotection by dietary phenolics against melanogenesis induced by UVA through Nrf2-dependent antioxidant responses. Redox Biol. 2016; 8:79–90. [PubMed: 26765101]

17. Schafer M, Werner S. Nrf2–A regulator of keratinocyte redox signaling. Free Radic Biol Med. 2015; 88:243–252. [PubMed: 25912479]

18. Schafer M, Willrodt AH, Kurinna S, Link AS, Farwanah H, Geusau A, Gruber F, Sorg O, Huebner AJ, Roop DR, Sandhoff K, Saurat JH, Tschachler E, Schneider MR, Langbein L, Bloch W, Beer HD, Werner S. Activation of Nrf2 in keratinocytes causes chloracne (MADISH)-like skin disease in mice. EMBO Mol Med. 2014; 6:442–457. [PubMed: 24503019]

19. Nys K, Maes H, Andrei G, Snoeck R, Garmyn M, Agostinis P. Skin mild hypoxia enhances killing of UVB-damaged keratinocytes through reactive oxygen species-mediated apoptosis requiring Noxa and Bim. Free Radic Biol Med. 2012; 52:1111–1120. [PubMed: 22245094]

20. Chaisiriwong L, Wanitphakdeedecha R, Sitthinamsuwan P, Sampattavanich S, Chatsiricharoenkul S, Manuskiatti W, Panich U. A case-control study of involvement of oxidative DNA damage and alteration of antioxidant defense system in patients with basal cell carcinoma: modulation by tumor removal. Oxid Cell Longev Med. 2016; 2016:5934024.

21. Johns EJ, O'Shaughnessy B, O'Neill S, Lane B, Healy V. Impact of elevated dietary sodium intake on NAD(P)H oxidase and SOD in the cortex and medulla of the rat kidney. Am J Physiol Regul Integr Comp Physiol. 2010; 2992:234–240.

22. Monk LS, Fagerstedt KV, Crawford RM. Superoxide dismutase as an anaerobic polypeptide: a key factor in recovery from oxygen deprivation in Iris pseudacorus? Plant Physiol. 1987; 85:1016–1020. [PubMed: 16665795]

23. Slominski A, Kim TK, Brozyna AA, Janjetovic Z, Brooks DLP, Schwab LP, Skobowiat C, JóŸwicki W, Seagroves TN. The role of melanogenesis in regulation of melanoma behavior: melanogenesis leads to stimulation of HIF-1a expression and HIF-dependent attendant pathways. Arch Biochem Biophys. 2014; 563:79–93. [PubMed: 24997364]

24. López-Camarillo C, Ocampo EA, Casamichana ML, Pérez-Plasencia C, Alvarez-Sánchez E, Marchat LA. Protein kinases and transcription factors activation in response to UV-radiation of skin: implications for carcinogenesis. Int J Mol Sci. 2012; 13:142–172. [PubMed: 22312244]

25. Hu Y, Ma Y, Wu S, Chen T, He Y, Sun J, Jiao R, Jiang X, Huang Y, Deng L, Bai W. Protective effect of cyanidin-3-O-glucoside against ultraviolet B radiation-induced cell damage in human HaCaT keratinocytes. Front Pharmacol. 2016; 7(7):301. [PubMed: 27656146]

26. Wäster PK, Ollinger KM. redox-dependent translocation of p53 to mitochondria or nucleus in human melanocytes after UVA- and UVB-induced apoptosis. redox-dependent translocation of p53 to mitochondria or nucleus in human melanocytes after UVA- and UVB-induced apoptosis. J Investig Dermatol. 2009; 129:1769–1781. [PubMed: 19158844]

27. Di Domenico F, Perluigi M, Foppoli C, Blarzino C, Coccia R, De Marco F, Butterfield DA, Cini C. Protective effect of ferulic acid ethyl ester against oxidative stress mediated by UVB irradiation in human epidermal melanocytes. Free Radic Res. 2009; 43:365–375. [PubMed: 19274591]

28. Zeng Q, Wang Q, Chen X, Xia K, Tang J, Zhou X, Cheng Y, Chen Y, Huang L, Xiang H, Cao K, Zhou J. Analysis of lncRNAs expression in UVB-induced stress responses of melanocytes. J Dermatol Sci. 2015; 81:53–60. [PubMed: 26596215]

29. G gotek A, Skrzydlewska E. The role of transcription factor Nrf2 in skin cells metabolism. Arch Dermatol Res. 2015; 307:385–396. [PubMed: 25708189]

30. Bivik CA, Andersson EB, Rosdahl IK. Wavelength-specific effects on UVB-induced apoptosis in melanocytes. A study of Bcl-2/Bax expression and keratinocyte rescue effects. Melanoma Res. 2005; 15:7–13. [PubMed: 15714115]

31. D'Orazio J, Jarrett S, Amaro-Ortiz A, Scott T. UV radiation and the skin. Int J Mol Sci. 2013; 14:12222–12248. [PubMed: 23749111]

32. Duval C, Régnier M, Schmidt R. Distinct melanogenic response of human melanocytes in mono-culture, in co-culture with keratinocytes and in reconstructed epidermis, to UV exposure. Pigment Cell Res. 2001; 14:348–355. [PubMed: 11601656]

33. Imokawa G. Autocrine and paracrine regulation of melanocytes in human skin and in pigmentary disorders. Pigment Cell Res. 2004; 17:96–110. [PubMed: 15016298]

34. Imokawa G, Yada Y, Miyagishi M. Endothelins secreted from human keratinocytes are intrinsic mitogens for human melanocytes. J Biol Chem. 1992; 267:24675–24680. [PubMed: 1280264]

35. Song X, Mosby N, Yang J, Xu A, Abdel-Malek Z, Kadekaro AL. alpha-MSH activates immediate defense responses to UV-induced oxidative stress in human melanocytes. Pigment Cell Melanoma Res. 2009; 22:809–818. [PubMed: 19659742]

36. Tada A, Suzuki I, Im S, Davis MB, Cornelius J, Babcock G, Nordlund JJ, Abdel-Malek ZA. Endothelin-1 is a paracrine growth factor that modulates melanogenesis of human melanocytes and participates in their responses to ultraviolet radiation. Growth Differ. 1998; 9:575–584.

37. Waster P, Rosdahl I, Öllinger K. Cell fate regulated by nuclear factor-κB- and activator protein-1-dependent signalling in human melanocytes exposed to ultraviolet A and ultraviolet B. Br J Dermatol. 2014; 171:1336–1346. [PubMed: 25046326]

38. Cagnol S, Chambard JC. ERK and cell death: mechanisms of ERK-induced cell death–apoptosis, autophagy and senescence. FEBS J. 2010; 277:2–21. [PubMed: 19843174]

39. Wada T, Penninger JM. Mitogen-activated protein kinases in apoptosis regulation. Oncogene. 2004; 23:2838–2849. [PubMed: 15077147]

40. Zhang W, Liu HT. MAPK signal pathways in the regulation of cell proliferation in mammalian cells. Cell Res. 2002; 12:9–18. [PubMed: 11942415]

41. Shi Q, Zhang W, Guo S, Jian Z, Li S, Li K, Ge R, Dai W, Wang G, Gao T, Li C. Oxidative stress-induced overexpression of miR-25: the mechanism underlying the degeneration of melanocytes in vitiligo. Cell Death Differ. 2015; 23:496–508. [PubMed: 26315342]

42. López S, Smith-Zubiaga I, García de Galdeano A, Boyano MD, García O, Gardeazábal J, Martinez-Cadenas C, Izagirre N, de la Rúa C, Alonso S. Comparison of the transcriptional profiles of melanocytes from dark and light skinned individuals under basal conditions and following ultraviolet-B irradiation. PLoS One. 2015; 10:e0134911. [PubMed: 26244334]

43. Bubici C, Papa S, Dean K, Franzoso G. Mutual cross-talk between reactive oxygen species and nuclear factor-kappa B: molecular basis and biological significance. Oncogene. 2006; 25:6731–6748. [PubMed: 17072325]

44. Chen L, Xu B, Liu L, Luo Y, Yin J, Zhou H, Chen W, Shen T, Han X, Huang S. Hydrogen peroxide inhibits mTOR signaling by activation of AMPKalpha leading to apoptosis of neuronal cells. Lab Investig. 2010; 90:762–773. [PubMed: 20142804]

45. Gutiérrez-Uzquiza Á, Arechederra M, Bragado P, Aguirre-Ghiso JA, Porras A. p38α mediates cell survival in response to oxidative stress via induction of antioxidant genes: effect on the p70S6K pathway. J Biol Chem. 2012; 287:2632–2642. [PubMed: 22139847]

46. Ja czyk A, Garcia-Lopez MA, Fernandez-Peñas P, Alonso-Lebrero JL, Benedicto I, López-Cabrera M, Gonzalez S. A Polypodium leucotomos extract inhibits solar-simulated radiation-induced TNF-alpha and iNOS expression, transcriptional activation and apoptosis. Exp Dermatol. 2007; 16:823–829. [PubMed: 17845214]

47. Muthusamy V, Piva TJ. UVB-stimulated TNFα release from human melanocyte and melanoma cells is mediated by p38 MAPK. Int J Mol Sci. 2013; 14:17029–17054. [PubMed: 23965971]

48. Schäfer M, Willrodt AH, Kurinna S, Link AS, Farwanah H, Geusau A, Gruber F, Sorg O, Huebner AJ, Roop DR, Sandhoff K, Saurat JH, Tschachler E, Schneider MR, Langbein L, Bloch W, Beer HD, Werner S. Activation of Nrf2 in keratinocytes causes chloracne (MADISH)-like skin disease in mice. EMBO Mol Med. 2014; 6:442–457. [PubMed: 24503019]

49. Bowen AR, Hanks AN, Allen SM, Alexander A, Diedrich MJ, Grossman D. Apoptosis regulators and responses in human melanocytic and keratinocytic cells. J Investig Dermatol. 2003; 120:48–55. [PubMed: 12535197]

50. von Thaler AK, Kamenisch Y, Berneburg M. The role of ultraviolet radiation in melanomagenesis. Exp Dermatol. 2010; 19:81–88. [PubMed: 20067521]

Appendix A. Supporting information

Supplementary data associated with this article can be found in the online version at http://dx.doi.org/10.1016/j.freeradbiomed.2017.05.009.
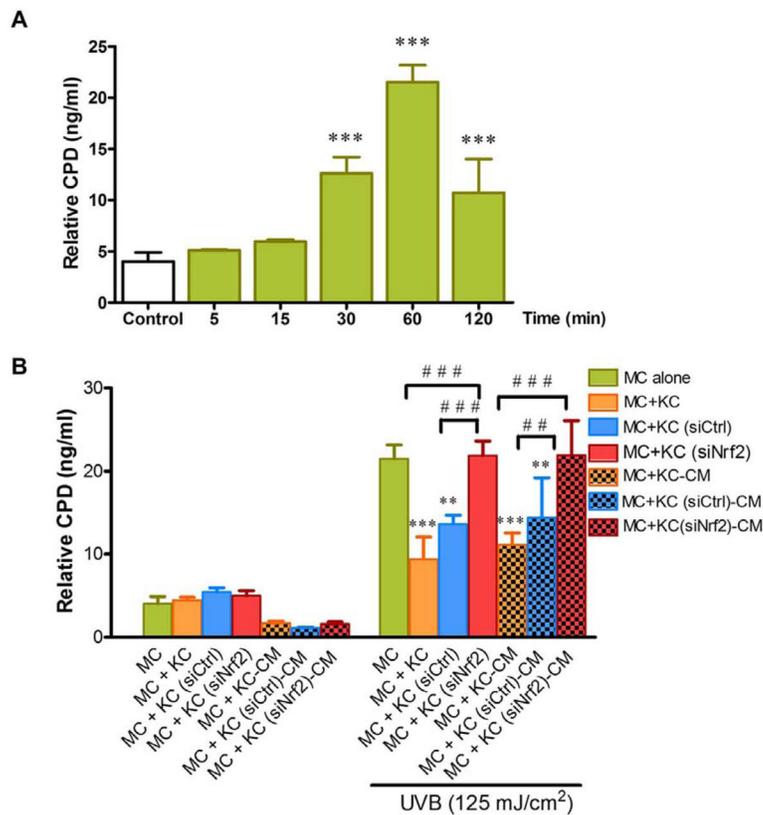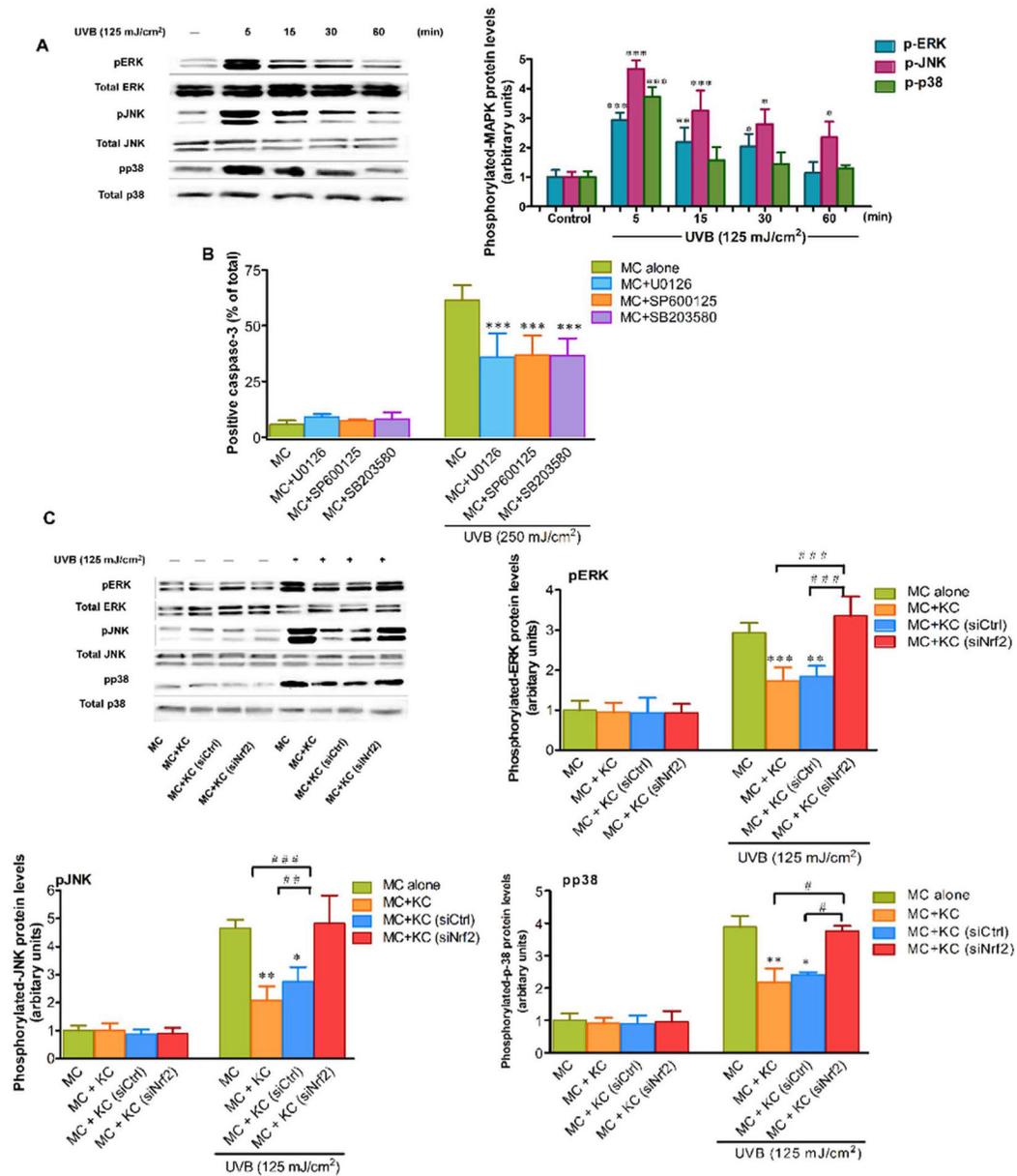
Fig. 1. The effects of Nrf2 knockdown in primary human keratinocytes (KC) on UVB-induced CPD formation in melanocytes (MC)

(A) Time-dependent effects of UVB (125 mJ/cm^2) on DNA damage (CPD) in MC. MC were collected after UVB (125 mJ/cm^2) irradiation at 5, 15, 30, 60 and 120 min. Data was expressed as mean ± SD. The statistical significance of differences was evaluated by one-way ANOVA followed by Dunnett's test. ***P < 0.001 versus unirradiated MC monoculture. (B) At 1 h after UVB (125 mJ/cm^2) irradiation, CPD formation was determined in MC monoculture, MC co-cultured in transwell with siNrf2 or siCtrl-transfected KC and MC pretreated with the CM from siNrf2 or siCtrl-transfected KC following UVB irradiation. Data were expressed as mean ± SD. The statistical significance of differences was evaluated by one-way ANOVA followed by Dunnett's test. **P < 0.01; ***P < 0.001 versus UVB-irradiated MC monoculture. ##P < 0.01; ###P < 0.001 versus UVB-irradiated MC+KC (siNrf2) or UVB-irradiated MC+KC (siNrf2)-CM.
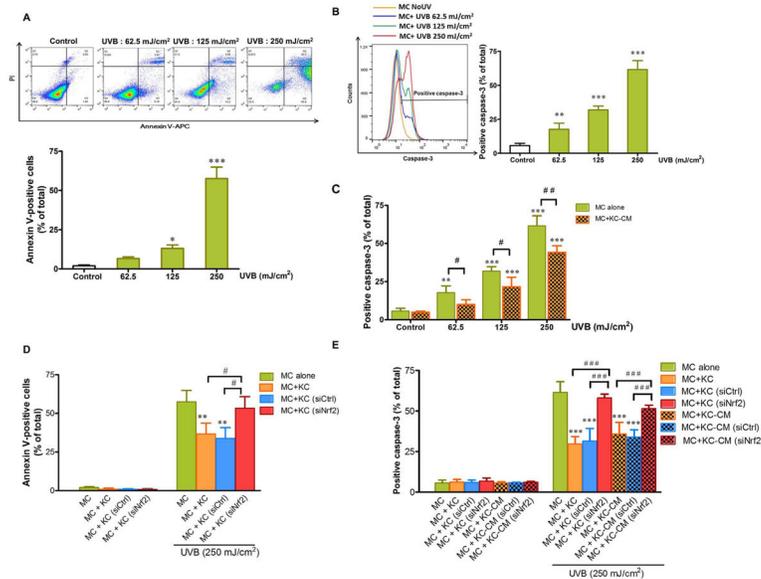
Fig. 2. The effects of Nrf2 knockdown in KC on UVB-induced apoptosis of MC
Dose-dependent effects of UVB on annexin V positivity (A) and active caspase-3 (B) in MC alone. The statistical significance of differences was evaluated by one-way ANOVA followed by Dunnett's test. $*P < 0.05$; $**P < 0.01$; $***P < 0.001$ versus unirradiated MC monoculture. (C) Dose-dependent effects of UVB on active caspase-3 in MC pretreated with CM from KC irradiated with UVB for 30 min. The statistical significance of differences between unirradiated MC and UVB-irradiated MC monoculture was evaluated by one-way ANOVA followed by Dunnett's test ($**P < 0.01$; $***P < 0.001$ versus unirradiated control MC) and between the UVB-irradiated MC monoculture and UVB-irradiated MC+KC-CM was evaluated by Student's t-test ($\#P < 0.05$; $\#\#P < 0.01$ versus UVB-irradiated MC monoculture). The effects of UVB (250 mJ/cm^2) on annexin V positivity (D) and active caspase-3 (E) in MC monoculture, MC co-cultured in transwell with siNrf2 or siCtrl-transfected KC and MC pretreated with the CM from siNrf2 or siCtrl-transfected KC following UVB irradiation. MC were harvested at 12 h after UVB irradiation for determination of annexin V/PI and active caspase-3 staining. Data were expressed as mean ± SD. The statistical significance of differences was evaluated by one-way ANOVA followed by Dunnett's test. $**P < 0.01$, $***P < 0.001$ versus UVB-irradiated MC monoculture. $\#P < 0.05$; $\#\#\#P < 0.001$ versus UVB-irradiated MC+KC (siNrf2) or UVB-irradiated MC+KC (siNrf2)-CM.
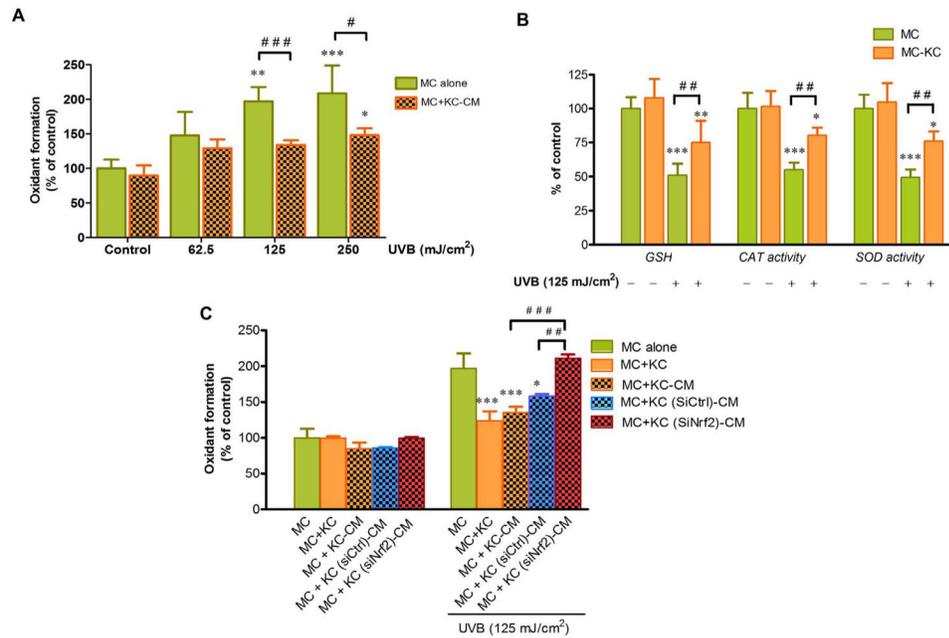
Fig. 3.
The effects of UVB-induced ROS formation and antioxidant defenses in MC co-cultured with KC: modulation by Nrf2 knockdown in KC. (A) Dose-dependent effects of UVB on oxidant formation in MC pretreated with CM from KC irradiated with UVB (62.5, 125 and 250 mJ/cm^2) for 30 min. The statistical significance of differences between unirradiated MC and UVB-irradiated MC monoculture was evaluated by one-way ANOVA followed by Dunnett's test (*P< 0.05; **P< 0.01; ***P< 0.001 versus unirradiated control MC) and between the UVB-irradiated MC monoculture and UVB-irradiated MC+KC-CM was evaluated by Student's t-test (#P< 0.05; ###P< 0.001 versus UVB-irradiated MC monoculture). (B) GSH levels and activities of catalase and SOD were determined at 1 h after UVB (125 mJ/cm^2) irradiation using a spectrofluorometer. The statistical significance of differences between unirradiated MC and UVB-irradiated cells was evaluated by one-way ANOVA followed by Dunnett's test (*P< 0.05; **P< 0.01; ***P< 0.001 versus unirradiated control MC) and between the UVB-irradiated MC monoculture and UVB-irradiated MC+KC was evaluated by Student's t-test (##P< 0.01 versus UVB-irradiated MC monoculture). (C) The effects of UVB (125 mJ/cm^2) on oxidant formation in MC monoculture, MC co-cultured in transwell with siNrf2 or siCtrl-transfected KC and MC pretreated with the CM from siNrf2 or siCtrl-transfected KC following UVB irradiation. The statistical significance of differences was evaluated by one-way ANOVA followed by Dunnett's test. *P< 0.05; ***P< 0.001 versus UVB-irradiated MC monoculture. ## P< 0.01; ###P< 0.001 versus UVB-irradiated MC+KC (siNrf2)-CM.

Fig. 4. The effects of Nrf2 knockdown in KC on UVB-mediated MAPK signaling in MC
(A) Time-dependent effects of UVB on MAPK phosphorylation in MC. MC were collected after UVB (125 mJ/cm²) irradiation at 5, 15, 30 and 60 min. Western blotting was performed to measure levels of p-ERK, p-JNK and p-p38 detected at 42, 54 and 38 kDa, respectively. The protein expressions were normalized to expression of loading controls; total ERK protein for p-ERK, total JNK protein for p-JNK and total p38 for p-p38. The statistical significance of differences was evaluated by one-way ANOVA followed by Dunnett's test. *P < 0.05; **P < 0.01; ***P < 0.001 versus unirradiated MC monoculture. (B) Active caspase-3 was determined in MC pretreated with 1 μM of specific ERK inhibitor (U0126), JNK inhibitor (SP600125) or p38 inhibitor (SB203580) for 1 h before UVB (250 mJ/cm²) irradiation. The statistical significance of differences was evaluated by one-way ANOVA

followed by Dunnett's test. ***P< 0.001 versus UVB-irradiated MC in the absence of the inhibitors. (C) The effects of UVB on p-ERK, p-JNK and p-p38 in MC monoculture and MC co-cultured with siNrf2 or siCtrl-transfected KC. MC were collected after UVB (125 mJ/cm^2) irradiation at 5 min. The statistical significance of differences was evaluated by one-way ANOVA followed by Dunnett's test. *P< 0.05; **P< 0.01; ***P< 0.001 versus UVB-irradiated MC monoculture. #P< 0.05; ##P< 0.01; ###P< 0.001 versus UVB-irradiated MC+KC (siNrf2).
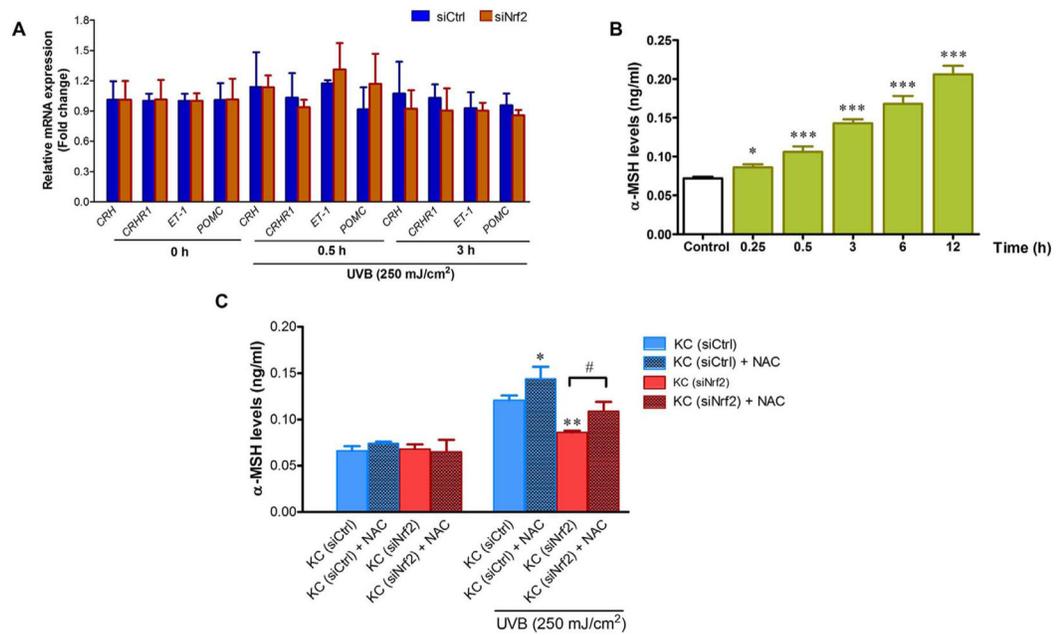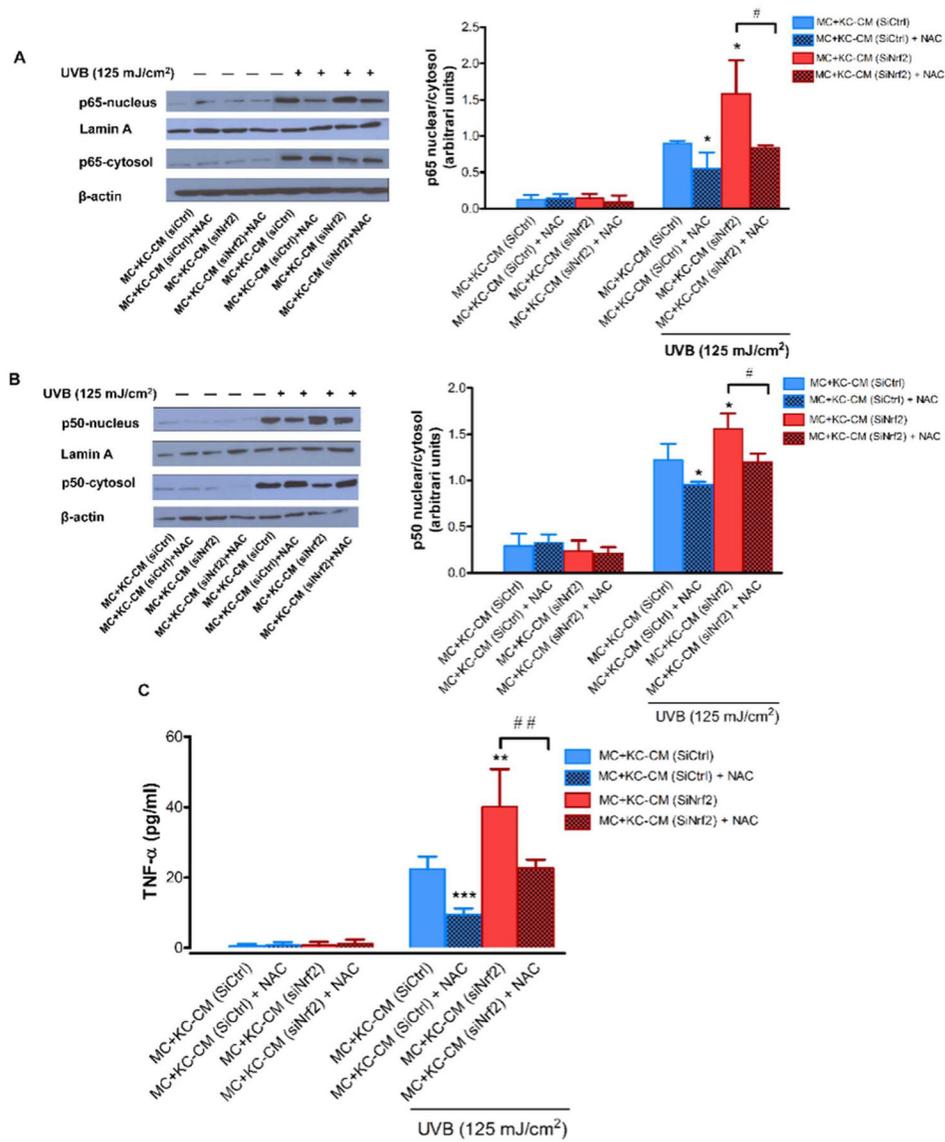
Fig. 5. Involvement of Nrf2 in the modulation of paracrine factor α-MSH produced by KC is ROS-dependent

(A) The effects of UVB (250 mJ/cm^2) on mRNA levels of the paracrine factors (ET-1, CRH, CRHR1 and POMC) at 30 min and 3 h post-irradiation in siCtrl- and siNrf2-transfected KC. The statistical significance of differences was evaluated by one-way ANOVA followed by Dunnett's test. (B) Time-dependent effects of UVB (250 mJ/cm^2) on α-MSH levels in CM from KC. KC were harvested at 0.25, 0.5, 3, 6 and 12 h after UVB irradiation. The statistical significance of differences was evaluated by one-way ANOVA followed by Dunnett's test. *$P < 0.05$; ***$P < 0.001$ versus unirradiated KC. (C) The effects of NAC treatment on UVB-induced α-MSH levels in CM from siCtrl and siNrf2-transfected KC. α-MSH levels in CM from siCtrl and siNrf2-transfected KC with or without NAC pretreatment were determined at 30 min following UVB exposure. The statistical significance of differences was evaluated by one-way ANOVA with Tukey's post hoc test. *$P < 0.05$; **$P < 0.01$ versus irradiated KC (siCtrl). #$P < 0.05$ versus UVB-irradiated KC (siNrf2) without NAC pretreatment.
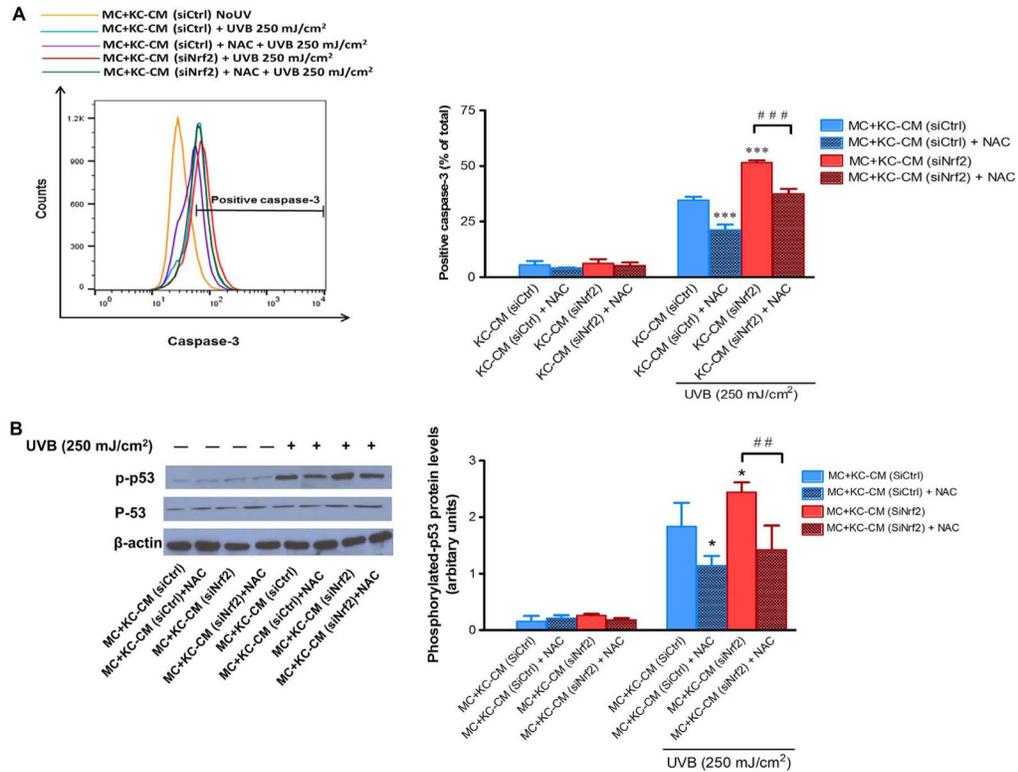
Fig. 6. Involvement of Nrf2 in the modulation of paracrine effect of KC on apoptosis is ROS-dependent

The effects of UVB (250 mJ/cm^2) on active caspase-3 (A) and phosphorylation of p53 (B) in MC incubated with CM from Nrf2-depleted KC pretreated with NAC. siCtrl- and siNrf2-transfected KC were pretreated with 5 mM NAC in Medium 154 without HKGS for 24 h. MC were then incubated with the CM from siCtrl- and siNrf2-transfected KC with or without NAC pretreatment for 30 min. Detection of active caspase-3 in MC was carried out at 12 h post-irradiation and of phosphorylated p53 and p53 at 15 min post-irradiation. The phosphorylated p53 and p53 were detected at 53 kDa, β-actin, the loading control for phosphorylated p53, at 42 kDa. Data were expressed as mean ± SD. The statistical significance of differences was evaluated by Student's *t*-test. *$P < 0.05$; ***$P < 0.001$ versus irradiated MC+KC (siCtrl)-CM. ##$P < 0.01$; ###$P < 0.001$ versus UVB-irradiated MC+KC (siNrf2)-CM without NAC pretreatment.

Fig. 7. Involvement of Nrf2 in the modulation of paracrine effect of KC on inflammatory response is ROS-dependent

The effects of UVB (125 mJ/cm^2) on nuclear translocation of p65 (A) and p50 (B) NF-κB subunits and TNF-α release (C) in MC incubated with CM from Nrf2-depleted KC pretreated with NAC. Western blotting was performed to determine nuclear tranlocation of p65 and p50 NF-κB subunits at 6 h following UVB irradiation. The p65 and p50 NF-κB subunits were detected at 65 and 50 kDa, respectively, lamin A, the loading control for nuclear protein, at 69 kDa and β-actin, the loading control for cytosol protein, at 42 kDa. TNF-α levels were quantified at 24 h post-irradiation using an ELISA kit. Data were expressed as mean ± SD. The statistical significance of differences was evaluated by Student's *t*-test. *$P < 0.05$; **$P < 0.01$; ***$P < 0.001$ versus irradiated MC+KC (siCtrl)-CM.

#*P* < 0.05 ## *P* < 0.01 versus UVB-irradiated MC+KC (siNrf2)-CM without NAC pretreatment.